The multi-year comparisons of chlorophyll and sea ice in Greenland Sea and Barents Sea and their relationships with the North Atlantic Oscillation

Version of Record: https://www.sciencedirect.com/science/article/pii/S0924796322000501
Manuscript_81035182ff0aafea3d5319c14b2dcbb7

The multi-year comparisons of chlorophyll and sea ice in Greenland Sea and Barents Sea and their relationships with the North Atlantic Oscillation

Bo Qu [1*] and Albert J. Gabric[2]

1. School of Science, Nantong University, Nantong, 226019, China.
2. School of Environment and Science, Griffith University, Nathan, Qld, 4111, Australia

Abstract: The Arctic Ocean (AO) has experienced very significant warming in recent decades with clear impacts on the extent and depth of sea ice cover. Sea ice serves as a primary habitat and plays an important role in the AO marine food web. The surface distributions of chlorophyll_*a* (CHL), sea ice concentration (ICE), sea surface temperature (SST) and North Atlantic Oscillation (NAO) are analyzed in the study region (20°W-50°E, 70°N-80°N) over the decade (2003-2014). This region spans the Barents Sea (BS), Norwegian (NS) and Greenland Sea (GS). In general, the peak of spatial averaged CHL in the BS was about 60% higher than the GS. Due to elevated SST in the southern BS, CHL was much higher especially in 2010 and 2013. In 2011, there was a strong meridional gradient in CHL decreasing from south to north of the BS, and also a strong zonal gradient from the southern GS to the southern BS. The northern GS had higher CHL than the southern GS due to the increased ice melting and nutrient-enriched runoff from east Greenland glaciers to the northern and western coastal regions of the GS. Seasonal peaks of spatially averaged CHL occurred in April or May and were about two weeks earlier in the BS than the GS. Higher ice melt in the northern BS was the main reason for CHL blooms especially in 2010 and 2011. Earlier and more extensive ice melting and a persistent negative NAO index causing atmospheric circulation patterns that favoured ice loss were the possible drivers of enhanced phytoplankton blooms in 2010. A previous negative winter NAO is thought to be linked to an increase in ICE in the following spring. NAO is mostly negative during spring in the GS. Sea ice melt was positively correlated with CHL in the northern sector of the study region.

Key words: Barents Sea, Greenland Sea, chlorophyll_*a*; sea ice， North Atlantic Oscillation (NAO)

1. INTRODUCTION

Climate change influences in the Arctic Ocean (AO) are considered to lead to significant impact on warming at the global scale. Findings from the IPCC indicate that the Arctic temperature has increased at almost twice the global average rate in the past 100 years. The Arctic sea ice extent is likely to further decline decline during the 21st century in response to atmospheric greenhouse gas loading (Stroeve et al. 2007, Zhang and Walsh 2006, Ardyna et al. 2014, Arrigo, van Dijken and Pabi 2008, Budikova 2009, Holland 2006, Struthers et al. 2011). Greenhouse warming in the Arctic leads to specific positive feedback loops in the region. The local surface albedo will significantly reduce due to the large amount of snow and ice melt. The surface area that used to reflect sunlight will now absorb it, resulting in more heat energy retained by the Earth's surface. In the AO, this will also mean changes in environmental factors such as SST and ocean mixed layer depth, and key ecological indicators such as phytoplankton biomass are likely to change accordingly.

The Barents Sea

The Barents Sea (BS) is a shallow marginal sea in the AO with the Norwegian Sea to its west and the Kara Sea to its east. The BS is well north of the Arctic Circle where the sun is always below the horizon during winter but constantly above the horizon during summer (Slagstad and Stole-Hansen 1991). From March to September, the mean fractional cloud cover is as high as 80% (Qu, Gabric and Matrai. 2006). Clouds and fog reduce sea surface incident light by about a half. The BS is a highly productive Arctic shelf sea and has experienced rapid and substantial climate-driven impacts on its marine ecosystem (Neukermans, Oziel and Babin 2018). It is also an important fishery region of the AO (Dalpadado et al. 2014), with the highest regional

primary and secondary production in the Arctic (Slagstad, Ellingsen and Wassmann 2011).

The Norwegian Atlantic Current transports warmer and saline waters northeastward into the BS from the southwest, which is mixed with the colder, southward flowing Arctic current from east of Svalbard (Harris, Plueddemann and Gawarkiewicz 1998). The Atlantic Current from the Norwegian Sea splits into two main branches in the BS, with one continuing eastwards parallel to the coastal current system and the other branch turning north to the west of Bear Island (Loeng 1991).

Intense phytoplankton blooms are reported every spring, supported by elevated winter stocks of nutrients which are supplied by vertical mixing and advection of Atlantic Water, with blooms also affected by the late onset of zooplankton grazing (Wassmann et al. 2006). The spring blooms are mainly composed of diatoms and Phaeocystis *pouchetii* (Engelsen et al. 2002, Kogeler and Rey 1999, Oziel et al. 2017, Wassmann 1999). The summer algal community is dominated by coccolithophores, among which Emiliana *huxleyi* is the most abundant and widespread species (Oziel et al. 2017, Neukermans et al. 2018). Coccolithophores are the most productive calcifying organism on Earth and are important components of the carbon cycle response to changes in atmospheric CO_2 level (Signorini and McClain 2009).

The Greenland Sea

The Greenland Sea (GS) is one of the few areas in the world's oceans where deep convective mixing occurs, a result of the complex physical processes when warmer and higher salinity North Atlantic waters flowing from the south mix with the colder and less saline Arctic waters from the north. The recirculation zone is within the Fram Strait (Figure 1). Therefore, during deep convection periods, significant amounts of carbon dioxide can be transported to great depth, a key process for global climate (Rey, Noji and and Mille 2000).

Similar to the BS, the spring phytoplankton community is composed mainly of diatoms and Phaeocystis *pouchetii* as dominant species or in mixed populations in the central Greenland Sea (Rey et al. 2000). In the North East polynya of the Greenland

Sea , diatom blooms start in April in the open waters and adjacent marginal ice zones, coupled with low biomass of flagellates under pack-ice (Gradinger and Baumann 1991, Lara 1994). These blooms almost deplete the nutrients, especially nitrate, in the euphotic zone (Spies 1987, Lara 1994). The upper water column is affected by melt waters from land runoff and sea ice. The lower layer shows characteristics of Arctic intermediate waters. Below 150m, the influence of the North Atlantic current with warmer and more saline waters can be recognized (Lara 1994).

North Atlantic Oscillation (NAO)

The NAO index is the pressure difference between two fixed locations near Iceland and the Azores (Hurrell 2000). The NAO refers to a redistribution of air masses between the Arctic and the subtropical Atlantic, with swings from one phase to another producing large changes in surface air temperature, winds, storminess and precipitation over the Atlantic as well as the adjacent continents (Hurrell and Deser 2009). A positive NAO indicates a northward shifting of the surface sea-level pressure with an enhanced zonal circulation regime (Glowienka-Hense 1985). Hence, a positive NAO phase in the Arctic Ocean can lead to lower than average ICE in association with increased temperatures related to enhanced atmospheric and oceanic heat transport (Liu, Curry and Hu 2004, Wang and Ikeda 2000, Yamamoto 2006) During positive NAO phases, almost the complete northern Eurasian continent is warmer than normal. High positive NAO causes an northward transport of pressure that warms the subpolar gyre and cools the subtropical one, and vice versa (D'Andrea, Czaja and Marshall 2005). Changes in the NAO can also influence regional phytoplankton dynamics (Dickman 1998). Dickman (1998) concluded that in the North East Atlantic, a positive NAO is associated with increased westerly wind stress and increased precipitation. Stronger mixing (due to increased winds) and higher nutrient levels (due to increased river run-off) should favour diatoms to the detriment of flagellates (Irigoien et al. 2000). Strong and Magnusdottir (2011) report that there is a negative feedback between the NAO and ICE, whereby a positive NAO index

tends to produce negative sea ice anomalies in the Barents Sea, which in turn forces negative NAO. Marshall, Johnson and Goodman (2001) found that both thermohaline circulation and ocean gyres can play a role in coupled interactions with the NAO on decadal timescales. Hurrell (1996) indicated that nearly all the cooling and warming in the north Atlantic and across Europe and Eurasia since the mid-1970 resulted from changes in NAO. Hence, the NAO is closely related to the local climate in the Arctic Ocean.

Research done to date has focused on CHL and its relationship with ICE in either the BS or GS, but has not compared the two regions. Here we divide the overall study region (20°W - 50°E, 70°N-80°N) into zonal sections the Greenland Sea (20°W-10°E，70°N -80°N) (GS), the Norwegian Sea (10°E-30°E，70°N -80°N) (NS) and the Barents Sea (30°E-50°E，70°N -80°N) (BS) sectors. Decadal spatial average CHL in the GS, NS and BS are compared. Then we focus on the GS and BS, to discuss the relationships between CHL and ICE as well as the interannual variations of NAO and its impact on variability in CHL and ICE.

2. MATERIAL AND METHODS

Spatial average CHL in the study region (20°W -50°E, 70°N -80°N) (including GS, NS and BS) are derived for the period 2003 - 2014. The time series of CHL is retrieved from the MODISA (Aqua), Level-3, 8-day, mapped archive (https://oceancolor.gsfc.nasa.gov/). Weekly SST and surface wind speed (WIND) are retrieved from the Remote Sensing Systems (RSS) archive at (http://www.remss.com/). Weekly ICE is obtained from the database at http://iridl.ldeo.columbia.edu/SOURCES/.NOAA/.NCEP/.EMC/.CMB/.GLOBAL/.Reyn_SmithOIv2/ (Reynolds 2002). Ice melt is calculated by subtracting the current and previous week's ICE.

The Northern Atlantic Oscillation (NAO) 8-day data is obtained by averaging the

daily NAO data from the National Weather Service Climate Prediction Center: https://www.cpc.ncep.noaa.gov/products/precip/CWlink/pna/nao.shtml (van den Dool, Saha and Johansson 2000).

Map images used in this paper were produced by using the Giovanni online retrieval system (https://giovanni.gsfc.nasa.gov/giovanni), developed and maintained by the NASA GES DISC (Acker and Leptoukh 2007).

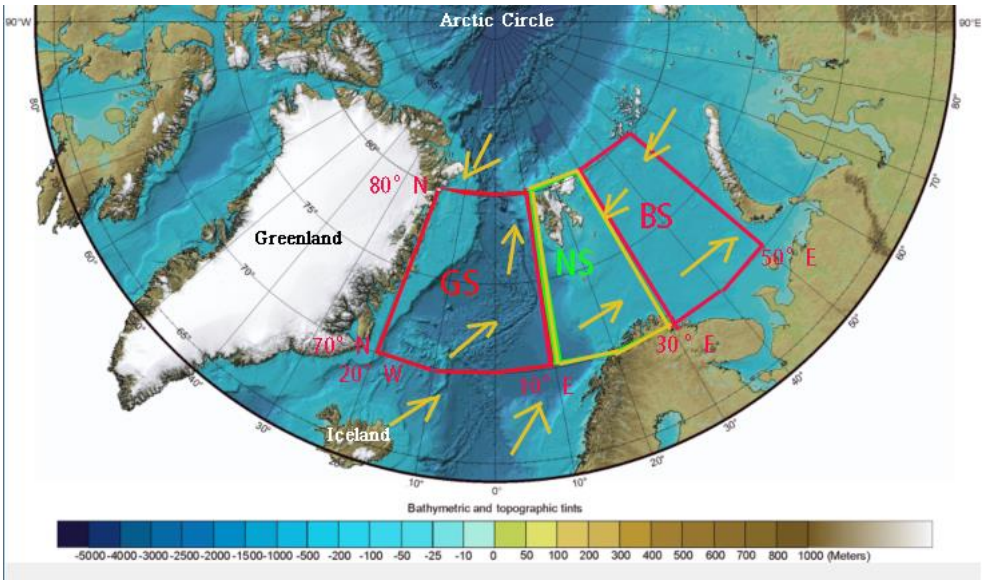

Fig. 1: Map of the study region. Greenland Sea (GS) and Barents Sea (BS) are enclosed in red frames and Norwegian Sea (NS) is enclosed in green frame. The yellow arrows indicate the surface current directions in and around the study region.

3. RESULTS

3.1 Regional CHL distribution

Annual spatial averaged CHL in the GS，NS and BS are shown for the period 2003-2014 in Figure 2(*a*). Spatial averaged CHL in the BS is generally higher than that in the GS. Spatial averaged CHL in the NS is within those in the BS and GS. The peak of CHL was in mid-April and was 8 days earlier in the BS (Figure 2a). The peak of CHL in BS was about 60% higher than that in GS. All secondary peaks occurred in late September, due to the regeneration of nutrients associated with decreased SST and increased wind in early fall (Hegseth 1997). Figure 2b shows the annual mean CHL time series for the GS and BS for their southern and northern regions. BSS refers to the southern region of BS, BSN refers to the northern of BS;

GSS refers to the southern region of GS, and GSN refers to the northern region of GS. Years 2010, 2011 and 2013（in BSS）had higher CHL peaks than other years. There was significant interannual variability in CHL in BSS. In 2011, the increase from BSN to BSS is 82%, and the increase from GSS to BSS is 187%. Year 2013 also presented a significant increase (around 126%) in BSS, compared to other regions. This was opposite to the meridional gradient in the BS where the southern spatial average CHL was much higher than that in the northern CHL. Spatial average CHL in GSS was only higher than that in GSN during 2006 and 2007, and lower in other years. The reasons for higher spatial average CHL in GSN in most years are discussed in Qu et al. (2016). However, compared to BS, there is no significant difference in spatial averaged CHL between GSS and GSN.

Annual mean CHL is compared between GS and BS for southern and northern regions in Figure 2c. Similar to Figure 2b, spatial averaged CHL in BSS had the highest concentration of the four regions. Peaks of CHL occurred in days 128 and 144 for BSS and BSN, respectively. The average time lag within the 12 years is 16 days. The peaks of CHL reached later in GS, at days 152 and 168 respectively for GSN and GSS. There were double peaks in GSN (at days 158 and 184, respectively).

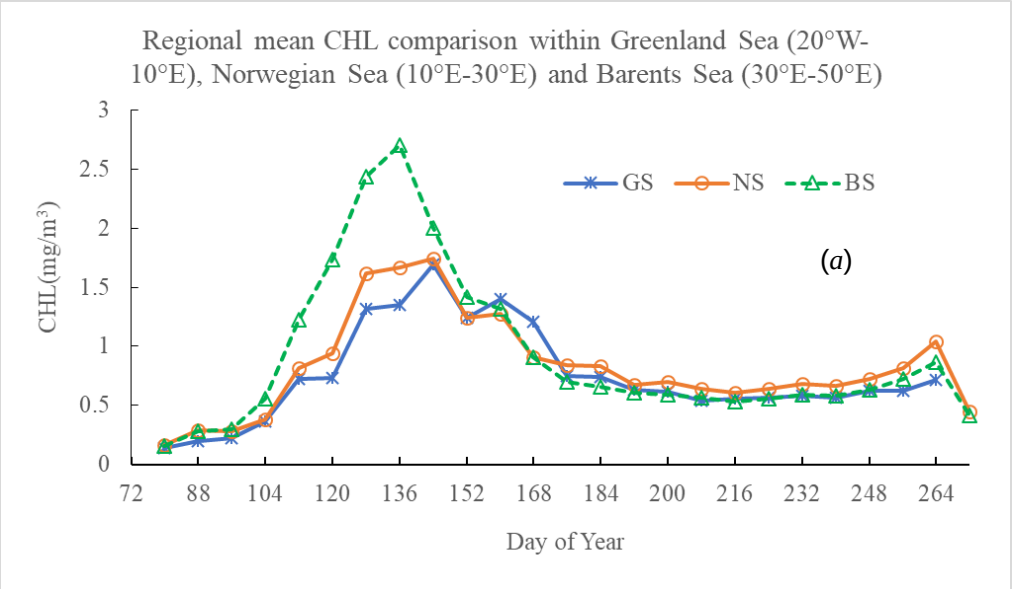

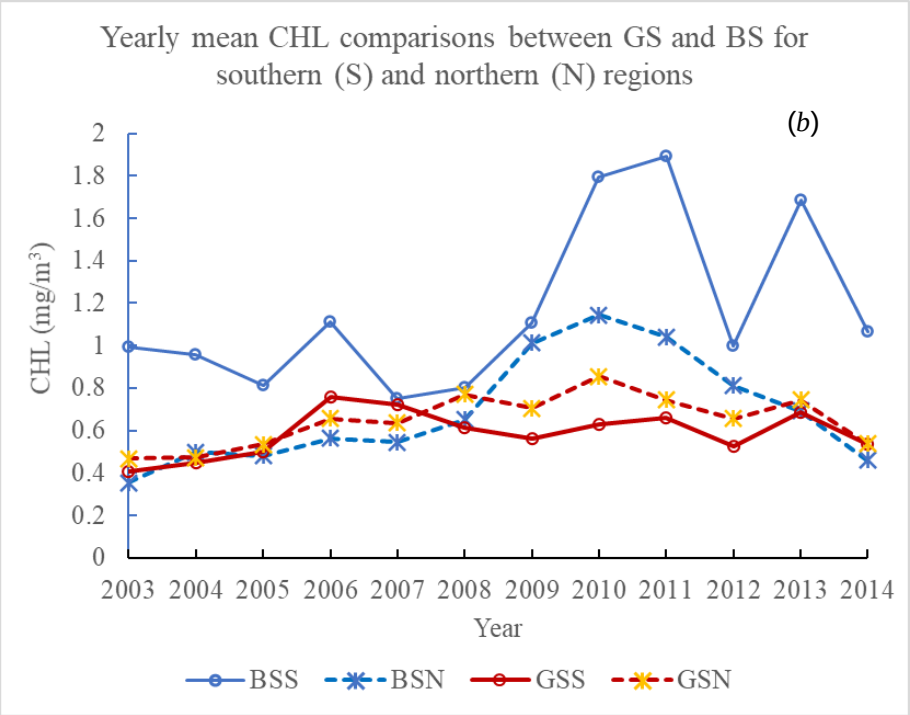

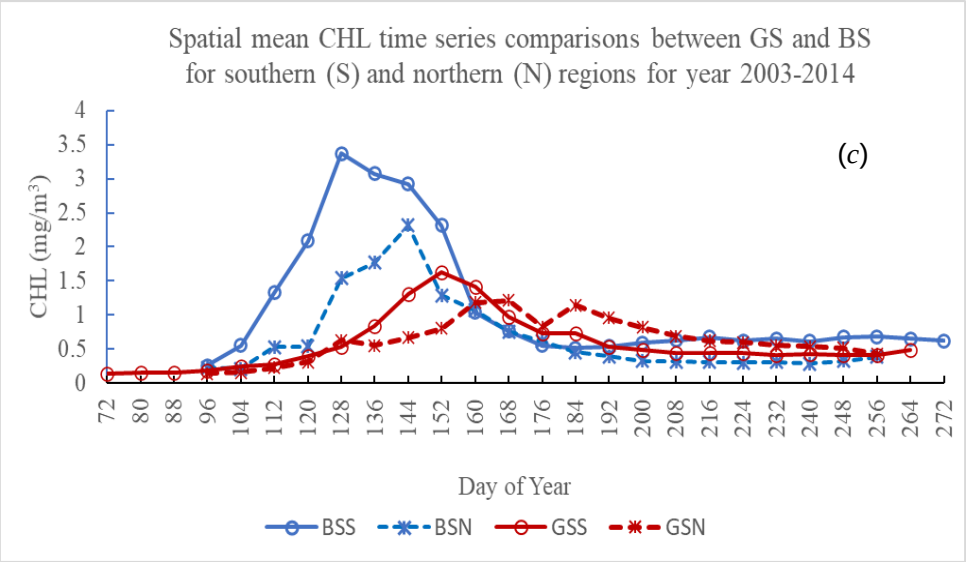

Fig. 2: (a) Regional spatial average CHL comparison within GS (20°W - 10°E, 70°N -80°N), NS (10°E - 30°E, 70°N - 80°N) and BS (30°E - 50°E, 70°N -80°N); (b) Yearly mean CHL comparisons among BSS, BSN, GSS and GSN; (c) Spatial average CHL time series comparisons between BSS, BSN, GSS and GSN averaged from year 2003 to 2014.

Time averaged CHL during the spring of 2010 is shown in Figure 3. The two vertical lines divide the study region into GS, NS and BS sub-regions. Phytoplankton blooms started in March in the eastern and southern regions of the BS. However, the bloom started in the northern region of the GS (Figure 3a). By mid-April, CHL reaches a maximum in both GS and BS (Figure 2c). Figure 3b shows the mean CHL

image for April-May during the vernal bloom period. Phytoplankton blooms spread out from the southwestern BS and then reached the northern region (Figure 3b). In the GS, blooms initiated in the western region near the east coast of Greenland. The Greenland glacial and river runoff plus nutrient discharge and increased water column stability in the coastal zone act to initiate the phytoplankton bloom (Moline et al. 2008). In May-June, the bloom started to decay in the BS but spread out in the northern region of GS and along the western coastline (Figure 3c).

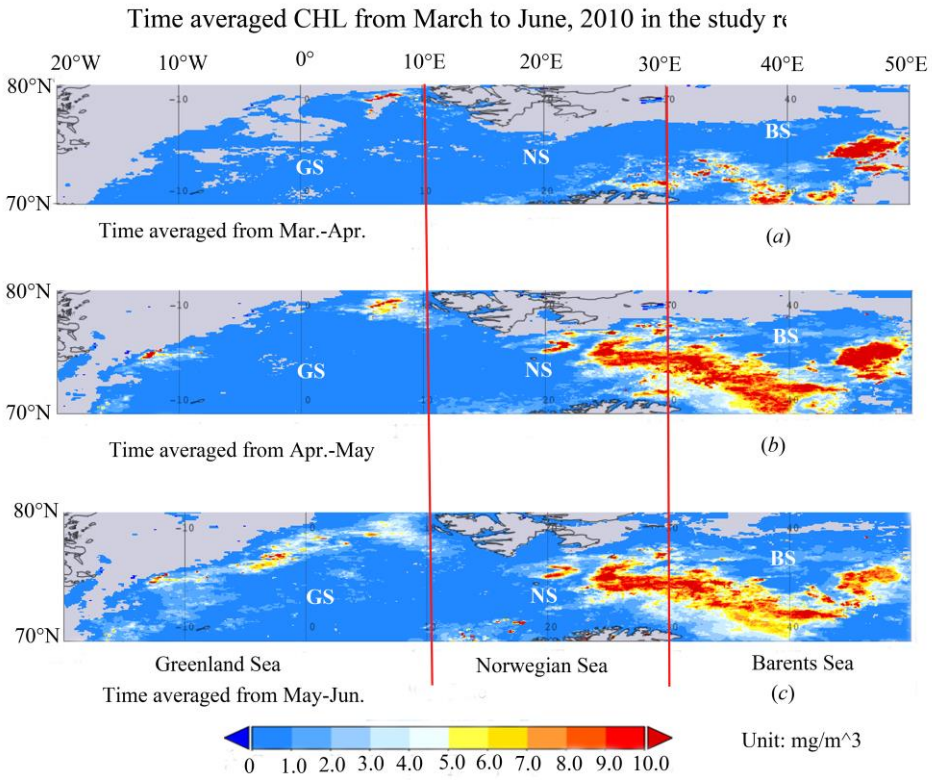

Fig. 3: Time averaged CHL in springtime of 2010 in the study region (a) March-April (b) April-May, and (c) May-June （https://giovanni.gsfc.nasa.gov/giovanni）.

In the southern region of the BS (Figure 4a), the spatial averaged CHL peaked on day 112 of 2011. Year 2010 had higher peaks than other years for both regions. Year 2013 had its earliest and the second highest peak on day 120 in the southern region. Table 1 lists the timing of the peak in spatial averaged CHL's for each year for both the southern and the northern regions. Much higher and earlier peaks appeared in the southern region, apart from year 2010. Year 2010 had the

221 highest peak. The top seven ranked peaks are observed in recent years.

222

223 **Table 1:** CHL regional average peak time and peak value for each year

	Southern Region		Northern Region		Rank
	Peak time (day)	Peak value (mg/m^3)	Peak time (day)	Peak value (mg/m^3)	For peak value
2003	144	5.03	136	0.91	
2004	128	3.54	144	2.56	
2005	152	2.93	152	1.70	
2006	120	4.28	152	2.09	
2007	152	2.18	152	1.98	
2008	144	2.75	144	2.64	
2009	152	6.34	160	3.43	5
2010	128	9.28	144	9.87	1
2011	128	7.52	128	6.93	2
2012	136	3.08	136	5.93	6
2013	120	8.53	144	2.04	3
2014	136	6.16	136	2.15	7

224

225 In general, the spatial averaged CHL was higher in the south and lower in
226 north in the study region. However, 2010 had its highest peak in the northern region
227 which was more than double that of other years apart from 2011 (Figure 4b in red).

228

229

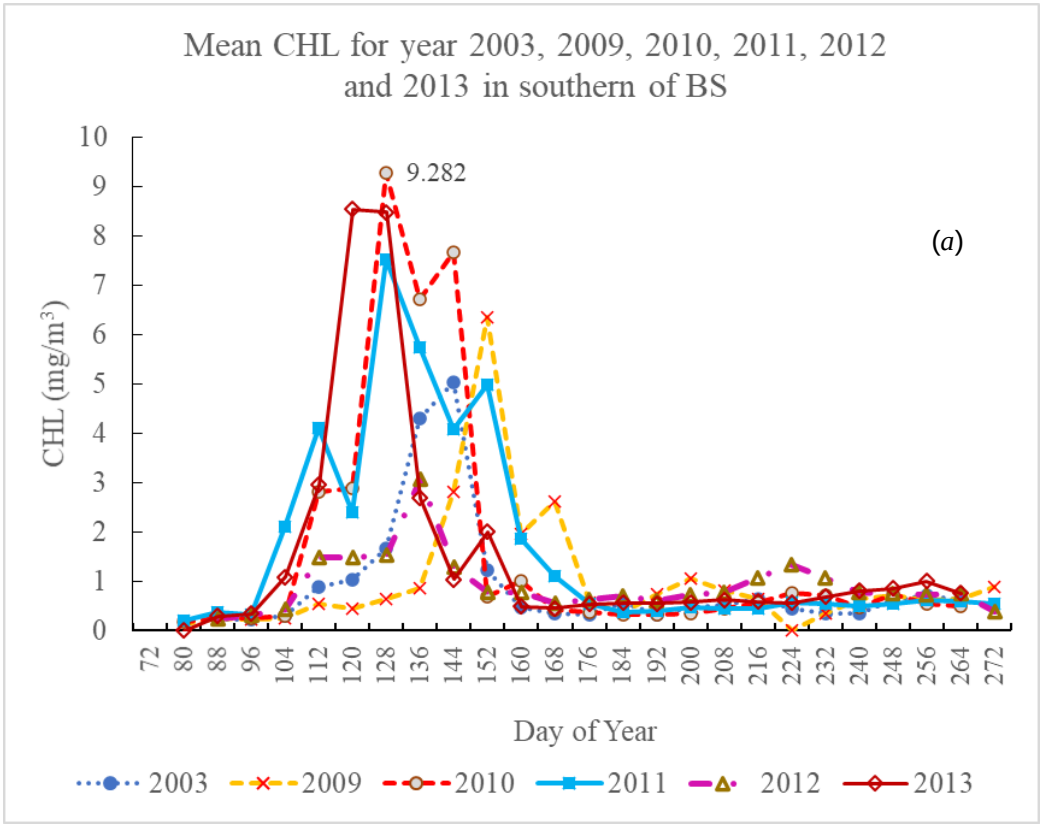

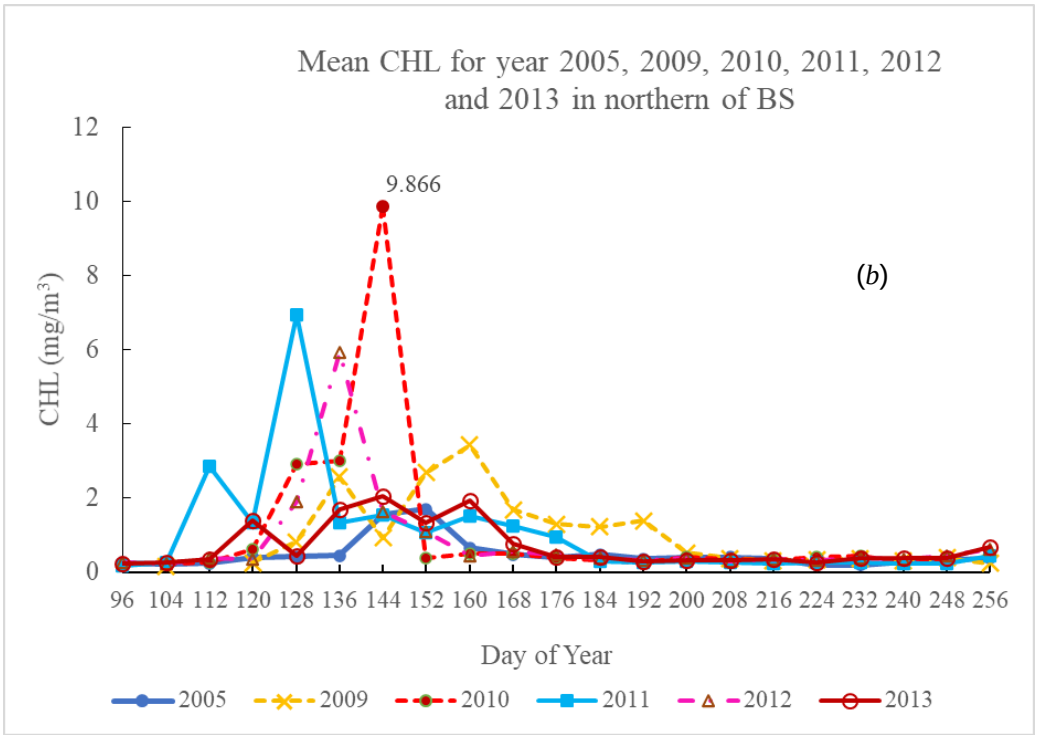

Fig. 4: Spatial average CHL in (a) southern study region of year 2003, 2009, 2010, 2011, 2012 and 2013; (b) northern study region for year 2005, 2009, 2010, 2011, 2012 and 2013.

We compared decadal spatial averaged CHL time series for 2003-2014 between GS and BS in the southern and northern study regions (Figure 5). BS (blue lines) had

its peaks on day 136 and GS had its peaks on day 144, 8 days later than BS. The significant elevated CHL in the south of BS is shown in the figure. Compared to the northern region, spatial average CHL increased 76.7% and 41.5% in southern region for BS and GS respectively. There were small second and third peaks in middle of July and middle August (day 224-232) in BS and a fourth peak on day 264 in late September.

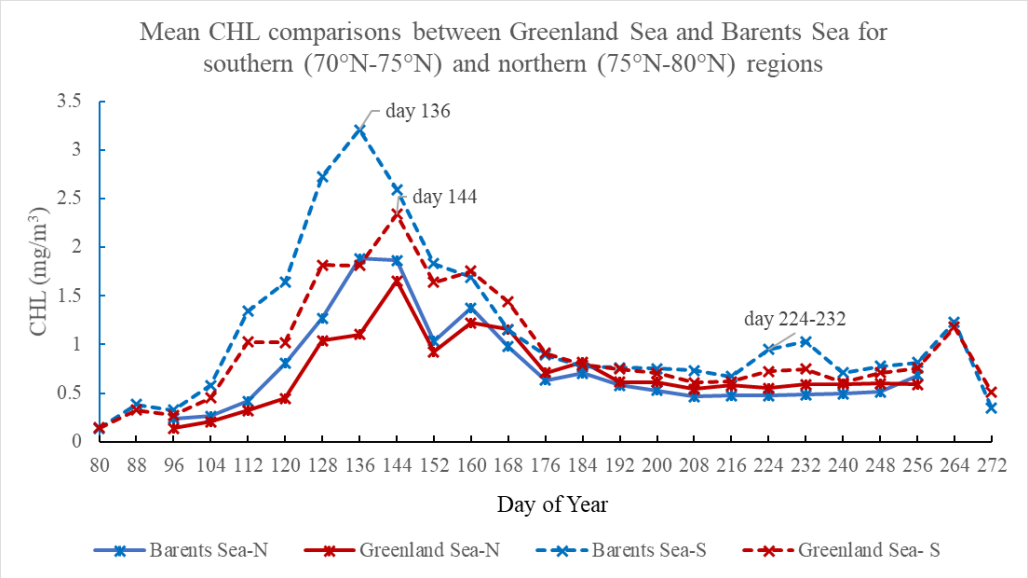

Fig. 5: Decadal apatial average CHL comparisons between Barents Sea and Greenland Sea. The dashed lines are the time series in southern region and solid lines are the ones in northern regions

There were significant increases in spatial averaged CHL in 2010 and 2013 in both the BS and GS. The spatial averaged CHL for the southern and northern regions are compared in Figure 6a and 6b. Compared to BSS and BSN, there were no significant differences on the CHL peak times in 2010 (Figure 6a). But there was a big shift of the CHL peak time in year 2013 (Figure 6b). when the peak (red curve) occurred around day 160 for both northern and southern regions in GS. In the BS (blue curve), the CHL peak shifted 16-24 days ahead in the northern region (day 144) compared to the southern region (day 120-128), with an increase of 59% in magnitude.

The reasons for elevated spatial average CHL in BS in 2010 and 2013 may be due to the earlier and more extensive sea ice melt in those years and a persistent

negative NAO index. In the GS, the increased runoff from glaciers on Greenland due to change of wind direction, possibly transporting nutrient enriched meltwater runoff from glaciers on eastern Greenland to northern coastal regions (Qu et al. 2016).

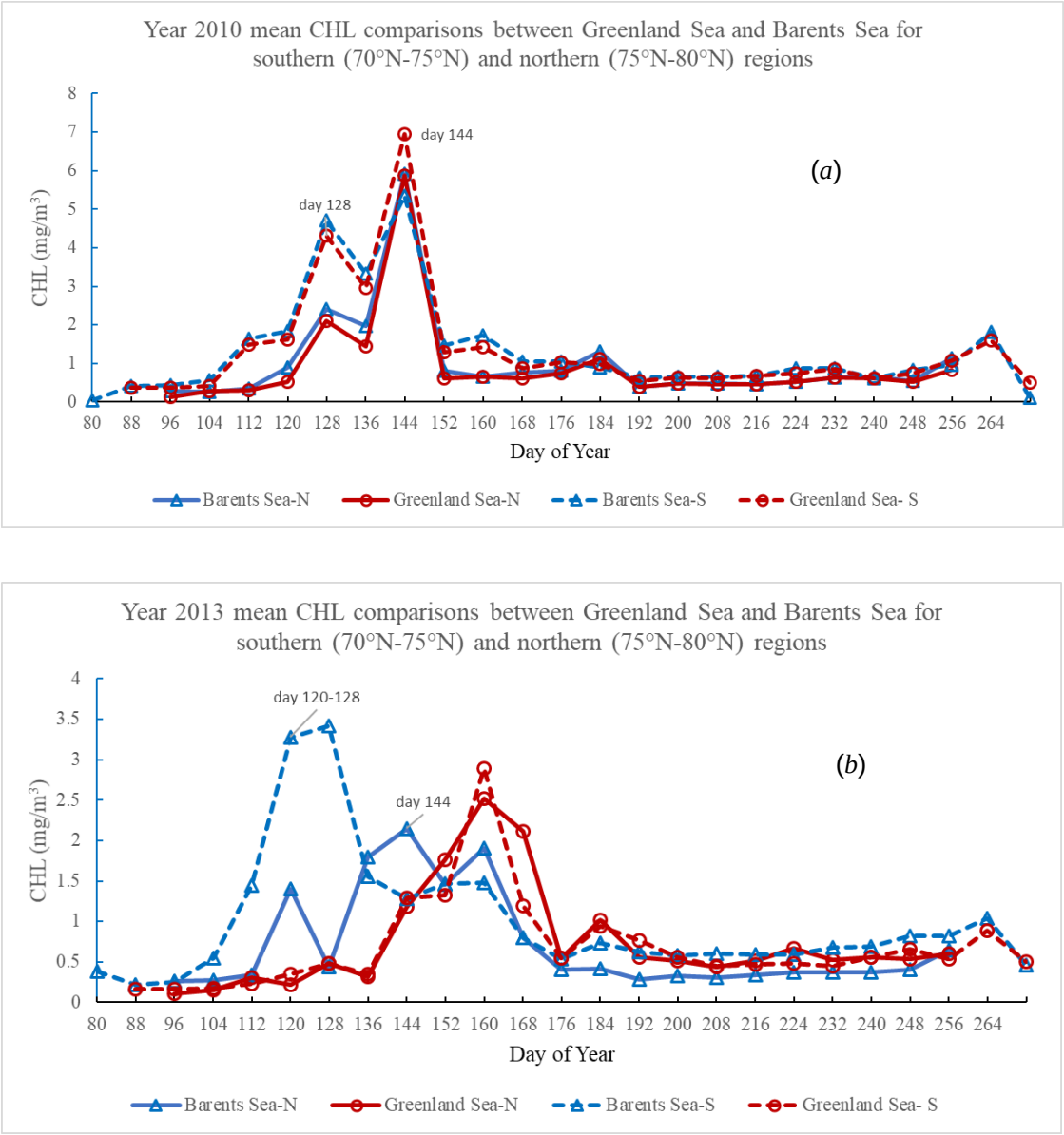

Fig. 6: Spatial average CHL comparisons between southern and northern region (a) for year 2010 and (b) for year 2013.

3.2 Sea ice cover (ICE)

Spatial averaged 8-day time series of ICE (ranging from 0-1) in the southern and northern regions of the GS and BS for 2003-2014 are shown in Figure 7a. In the northern region, spring ICE was higher in the BS and lower in the GS. After day 144, ICE decreased dramatically in the BS but was higher in GS. In the southern region,

spatial averaged ICE in the BS decreased under 4% in spring and almost disappeared after day 152. However, the southern region of the GS still had under 20% ICE and decreased to September. The ICE time series in the three regions (GS, NS and BS) is shown in Figure 7b. Year 2005 had a significant drop of ICE which was maintained at similar levels afterwards. The BS had higher spatial average ICE in early years (2003-2004), but lower than the GS after year 2005. Year 2010 saw higher ICE in the BS and GS while year 2013 saw higher ICE in GS. The BS saw significant ice loss during summer and southern region (Figure 7c), year 2010 had little more ICE during spring than other years, mostly covering the southeast part of BS (Figure 8a). Spatial averaged ICE has almost disappeared in recent years in BSS. In the BSN, spring ICE also reduced signifcantly after 2005. with a recovery in years 2009 and 2011.

BS has the largest open ocean area in the Arctic Ocean. The large amount of ice melt in its northern region is the major contribution to the phytoplankton biomass.

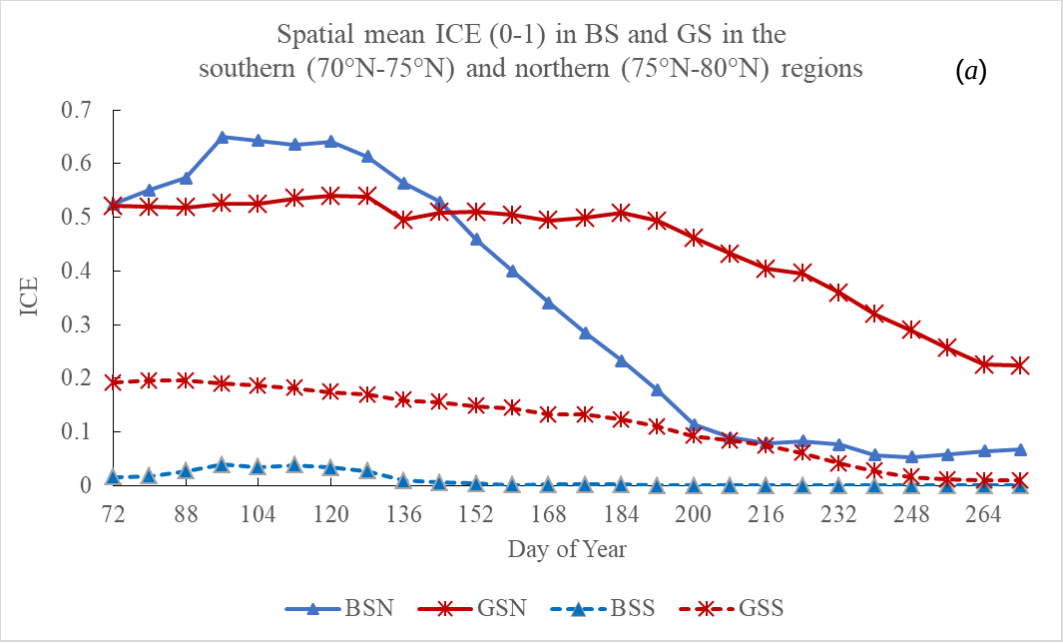

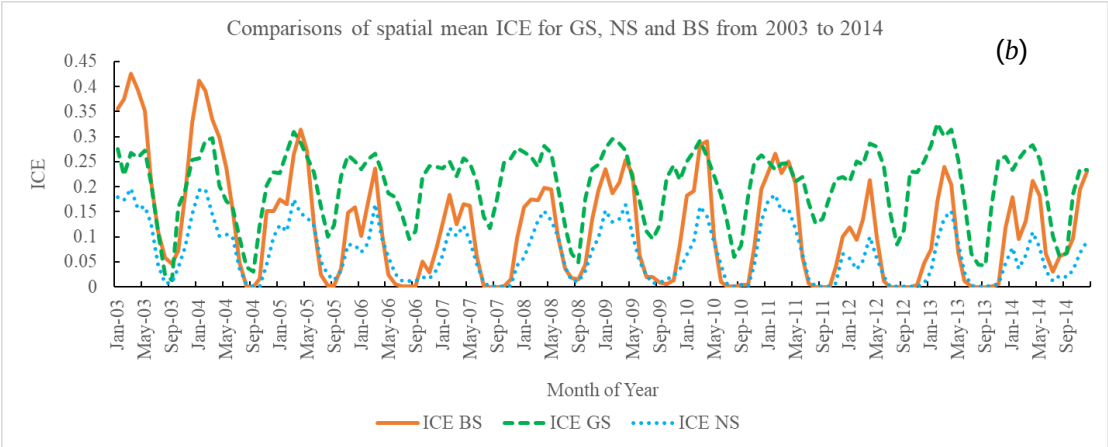

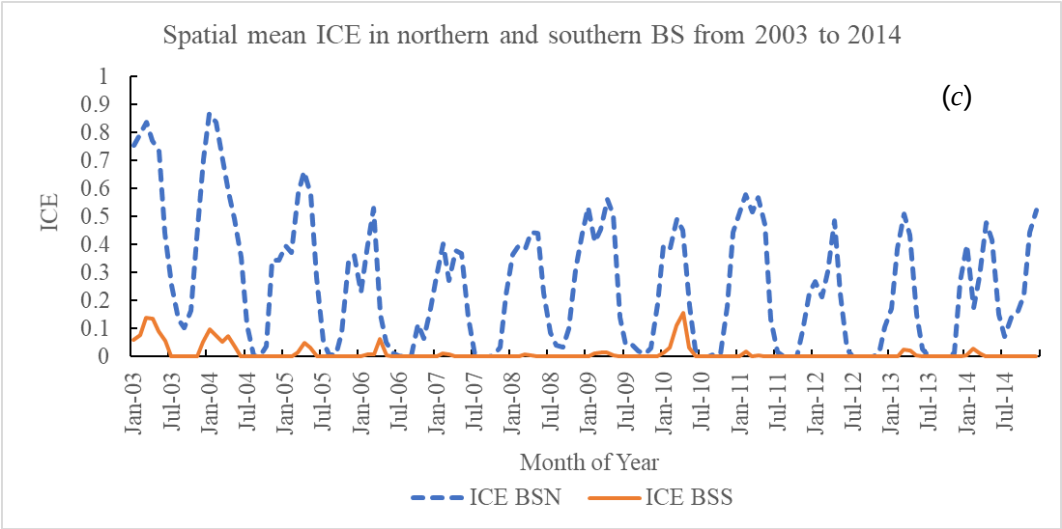

Fig. 7: (a) Spatial average ICE (range from 0 to 1) comparisons among GS, NS and BS; (b) Spatial average ICE time series for 12 years in the GS, NS and BS) for year 2003-2014. (c) Decadal spatial average ICE comparisons between Southern BS (BSS) and northern BS (BSN) for year 2003-2014.

The peak of ICE was during March-April in the west and northwest of GS, northeast of NS and northern and southeast of BS. ICE gradually decreased from May to June, especially in the northern BS. By July-August, sea ice almost disappeared in the BS with only a little left in the northwest of the GS.

Spatial averaged SST during 2003-2014 are compared in Figure 8a. SST in 2013 was higher than other years with 2003 recording the lowest SST. From 2003 to 2013, SST increased 140% in our study region (Figure 8a). Spatial averaged SST for the GS and BS in the southern and northern regions are compared for the period 2003-2014 (Figure 8b). The peak of SST occurred in July and there was a strong

meridional gradient in SST. The differences of SST between the southern and northern region were 0.52°C and 2.66°C for GS and BS, respectively.

Spatial average wind speed (WIND) was higher in winter and lower in summer (not show in figure). The spatial averaged WIND was 7.5 m/s in the study region. Winter WIND reaches 12m/s and summer WIND could be as low as 5m/s. The spatial average WIND in the northern region of BS was relatively higher than other regions.

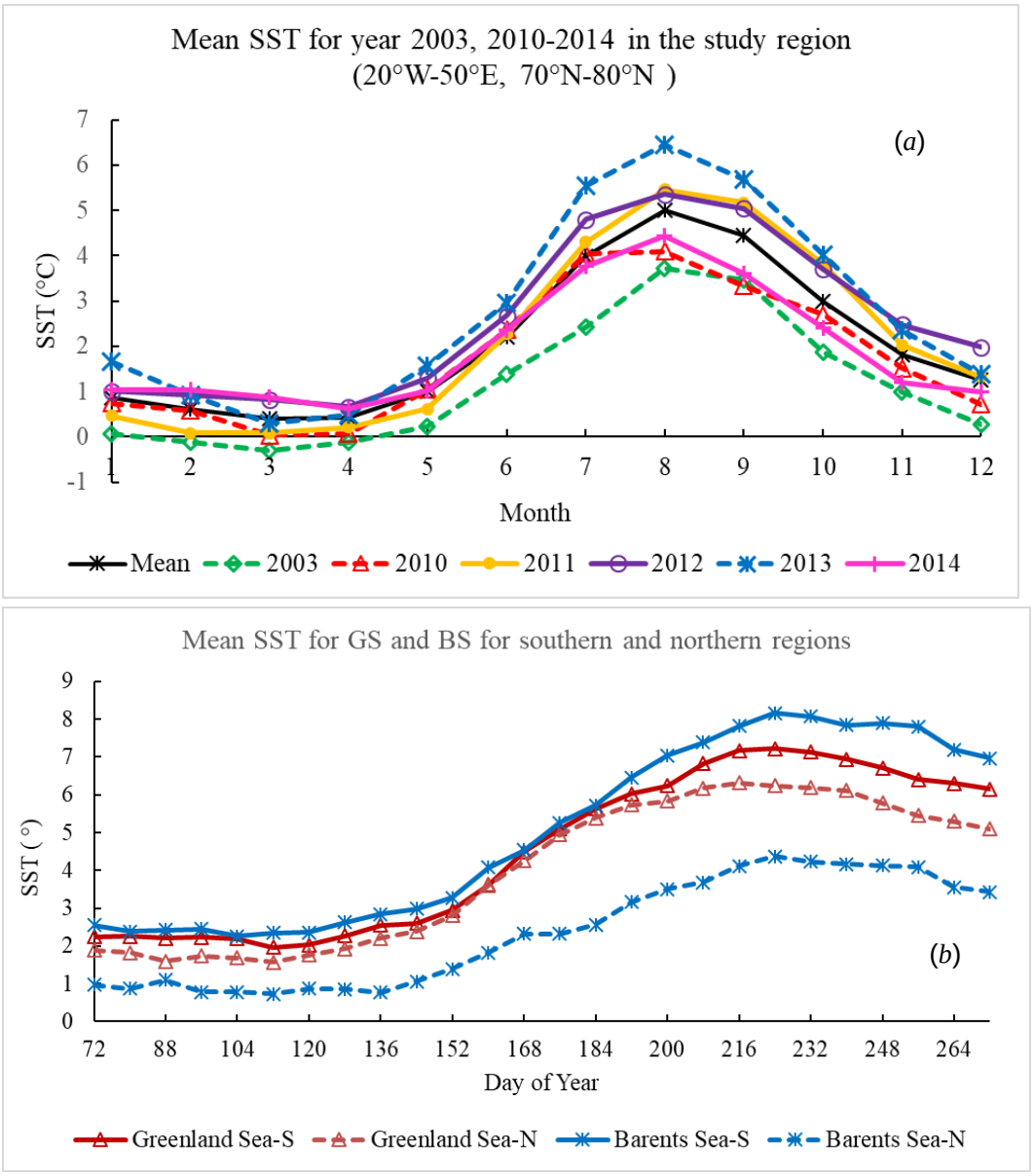

Fig. 8: (a) Decadal monthly spatial average SST comparison for year 2003, 2010-2014; (b) decadal 8-day spatial average SST comparisons for GS and BS of the northern and southern regions.

Three-monthly mean maps of SST for 2013 are shown in Figure 9. In season 1 (Jan.-Mar.), SST was relatively lower than other seasons. The intrusion of north Atlantic warm water from the southwest to the Arctic is clearly shown in Figure 9a. The first warm region was in the southeast of the GS and south of the NS. By the second season, the SST increase extended to the middle southern area (Figure 9b). By the third season of 2013, SST reached its peak（Figure 9c). Increased SST was evident over all the NS, most of the BS and part of the GS. The northern NS and northwest part of GS are still relatively cold. By the fourth season, SST decreased greatly, but was higher in the south, especially along the 0-40°E zonal region（Figure 9d）.

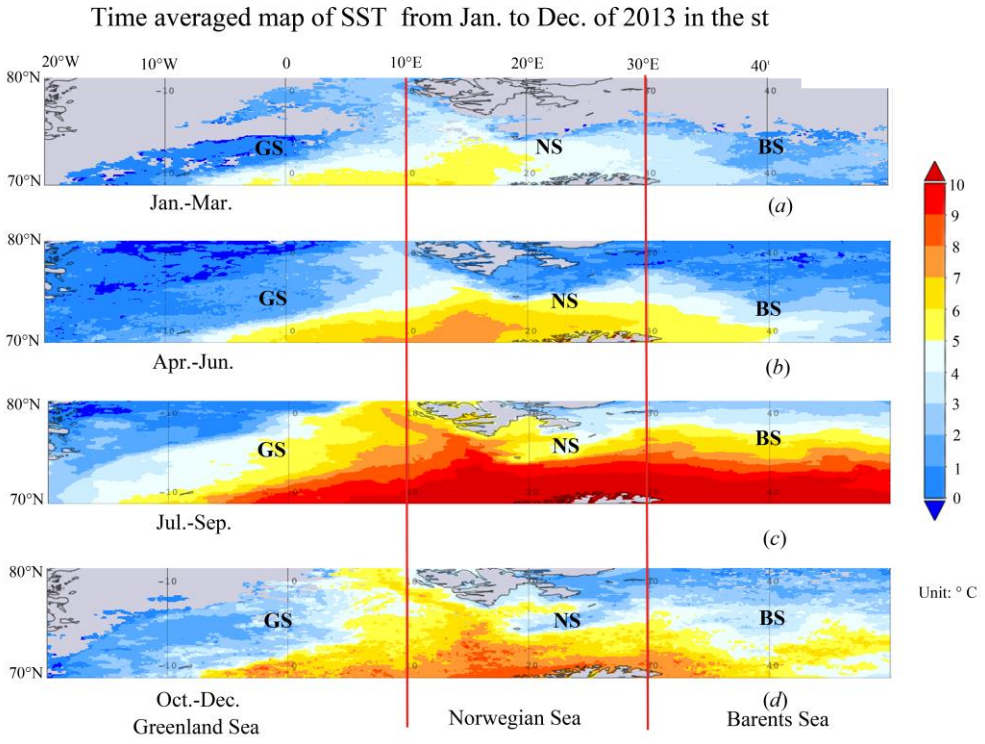

Fig. 9: Time averaged map of SST over year 2013 for different seasons: (a) for spring, (b) for summer, (c) for autumn and (d) for winter..

3.3 Correlations between NAO, CHL and ICE

3.3.1 The NAO index

Annual mean, together with spring mean NAO (MAM: averaged from day 96 to day 168) and winter mean (NDJ: averaged from day 320-365 and day 1 to day 31) are shown in Figure 10(a). During 2010 NAO was negative for the annual mean, spring

and winter means. Annual mean NAO tended to be positive during 2003-2004, and mostly negative during 2005-2010, then positive again in year 2011, 2013 and 2014. Spring NAO oscillated between positive and negative values during the entire study period. This phenomenon could be due to the interactions between ICE and WIND. During the spring season, sea ice melt is significant in the study region, especially in the north. Strong and Magnusdottir (2011) found that the NAO index is dependent on its coupling with area-averaged ICE in and around the Barents Sea. The coupling relationship exhibits negative feedback, whereby positive NAO tends to produce negative anomalies of ICE, which in turn forces negative NAO. Our zigzag pattern in the spring mean NAO supports their finding.

The detailed NAO time series (8-day interval) for year 2009, 2010 and 2011 is shown in Figure 10(b). Negative NAO started from the winter of 2009, and remained negative throughout most of 2010, becoming positive in 2011 during spring and winter. Year 2010 had extensive ice melting after March (Figure 8b, 8c for the BS), This phenomenon could be due to the strong negative NAO causing atmospheric circulation patterns that favoured sea ice loss (Strong and Magnusdottir 2011) and hence promoting the phytoplankton growth in 2010. The positive NAO during the winter of 2011 could lead to less ICE in the next year's spring. Hence, the positive NAO in the spring of 2011 (Figure 10b) corresponded with a reduction in ice melt and CHL concentration in 2012 (Figure 4a).

Year 2013 exhibited a negative NAO before the bloom season and positive NAO during the vernal blooming (MAM). The negative NAO during the bloom season caused less melt and higher ICE in the region. The rather elevated CHL in year 2013 was mainly because of a combination of warm SST (Figure 8a) and ice melt in the northern region. However, in the southern region (especially in the southern BS), ice almost disappeared in 2013. Elevated CHL in the southern region in 2013 was mainly caused by early warming (Figure 8a).

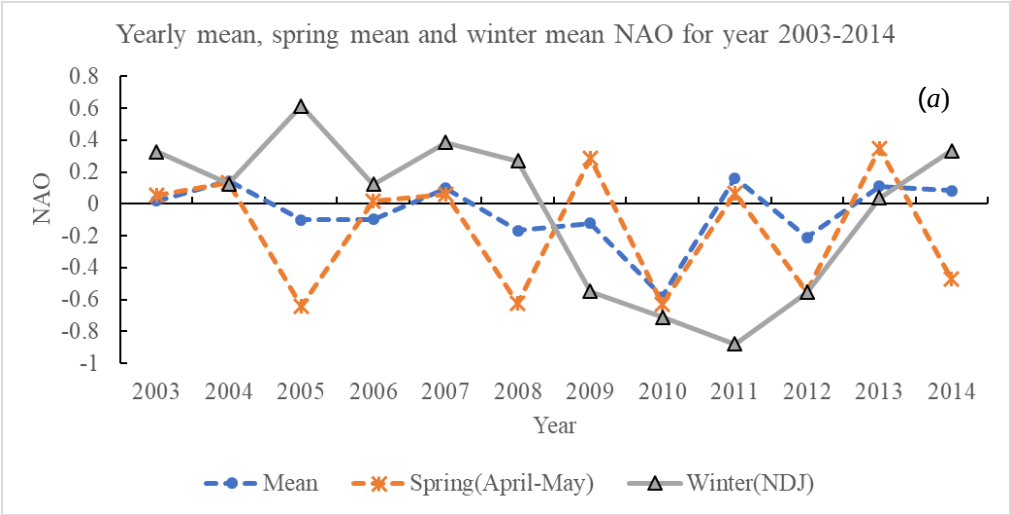

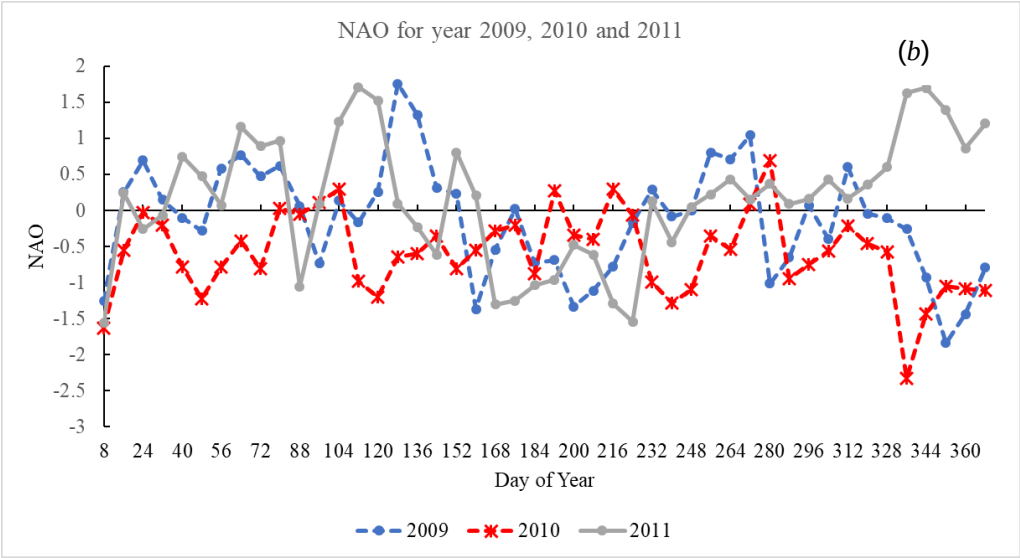

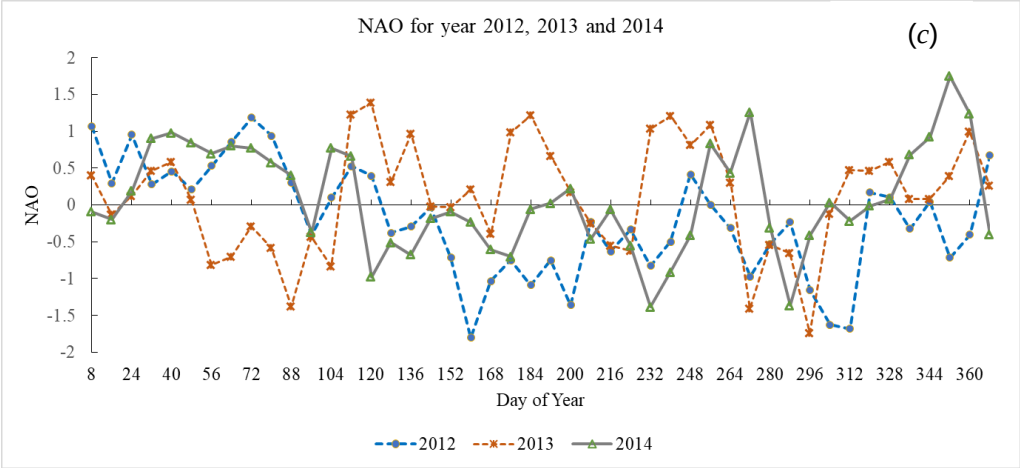

Fig. 10: (a) Yearly mean, spring mean and winter mean NAO for year 2003-2014; (b) 8-day time interval NAO for year 2009, 2010 and 2011; (c) 8-day time interval NAO for year 2012，2013 and 2014.

3.3.2 The correlation between NAO, CHL and ICE

The correlations of the previous winter's NAO and spring ICE in the northern region of BS and GS are shown in Figure 11a. The correlations are mostly negative. That means a previous winter negative NAO would indicate an increase in ICE in the following sprin.. The positive correlations in 2011 in BS and 2009 in GS could be due to the mismatch of the ice melt period we have used. The ice melting was much earlier in 2011 in the BS and much later in 2009.

We found there were more negative correlations between NAO and spatial average CHL in the GS (Figure 11b). The northern region of GS had even more negative NAO tendency. During March to May (MAM), there were more negative NAO indexes than the yearly mean. In the BS, mixed correlations occurred between NAO and spatial average CHL (not shown in figure). The reason is not clear.

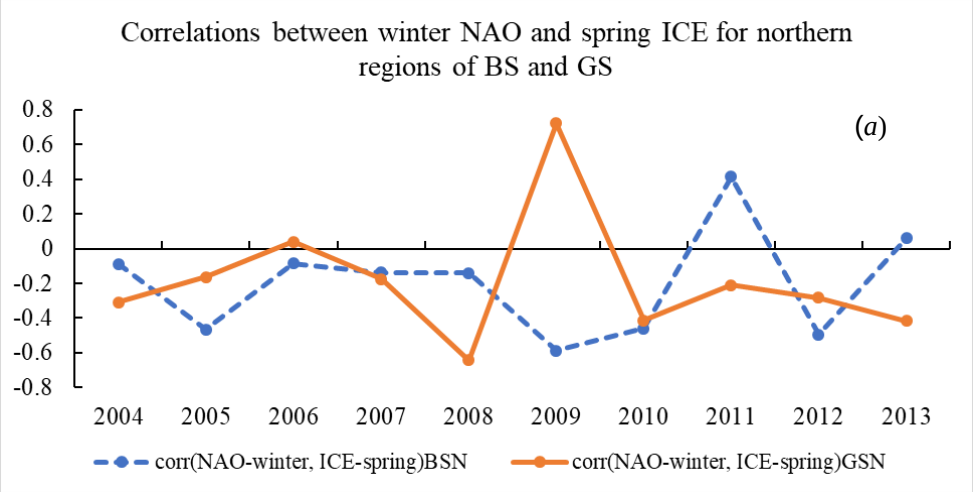

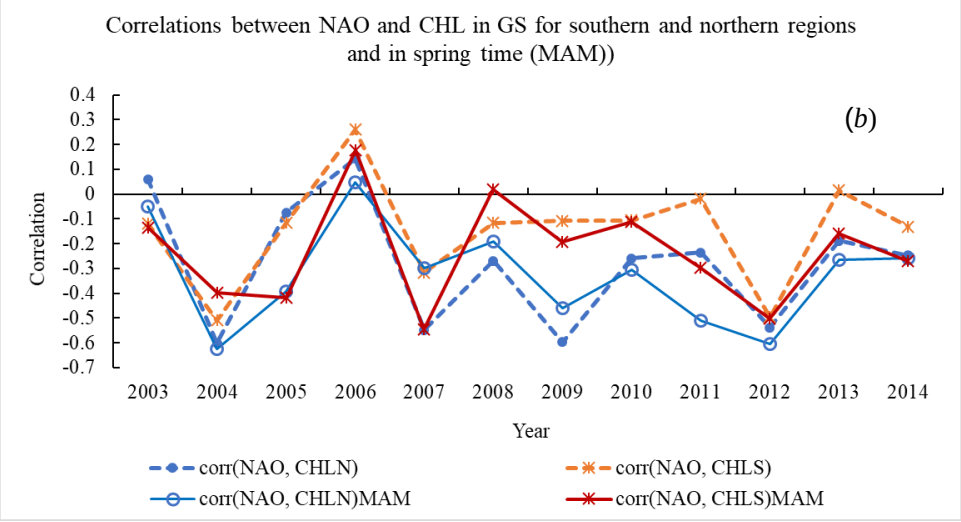

Fig. 11: (a) Correlations between previous winter NAO (NDJ) and spring ICE (April-May) in northern regions of BS and GS; (b) Correlations between NAO and spatial average CHL in GS for southern and northern regions as well as the springtime.

In general, spatial average CHL and ICE are negatively correlated in most years. ICE reached a peak about two months ahead of CHL in the GS and about one month ahead in the BS. It seems that NAO had a stronger influence in the GS rather than BS, due to its physical position. The melting ice, spatial averaged CHL in northern GS and NAO 8-day profile for 2010 are shown in Figure 12. The obvious positive correlations between melting ice and NAO as well as spatial average CHL in springtime (from day 96 to day 168) are evident. In the GS, the correlation between melting ice and NAO is 0.46. The correlation between melting ice and spatial average CHL is 0.54. For the period 2003-2014, spatial averaged CHL and melting ice had positive correlations of 0.4 (not shown in the figure). The melting ice corresponds with higher SST and increased phytoplankton biomass. This is consistent with our previous research results(Qu et al. 2014, Qu et al. 2016, Qu et al. 2006) as well as the research of Moline et al. (2008).

The following regression equations for CHL are obtained for southern and northern region of the GS by using EViews statistics software (Pang 2006):

CHL=0.266-0.054*NAO+0.021*ICE(-3); (for 20°W-10°E, 70°N -75°N) (3)

CHL=0.054-0.111*NAO-0.012*ICE(-3); (for 20°W-10°E, 75°N -80°N) (4)

Here ICE(-3) refers to the value ICE shifted three months behind, in order to have more close correlations with NAO and spatial average CHL. Equations (3) and (4) are also statistically significant.

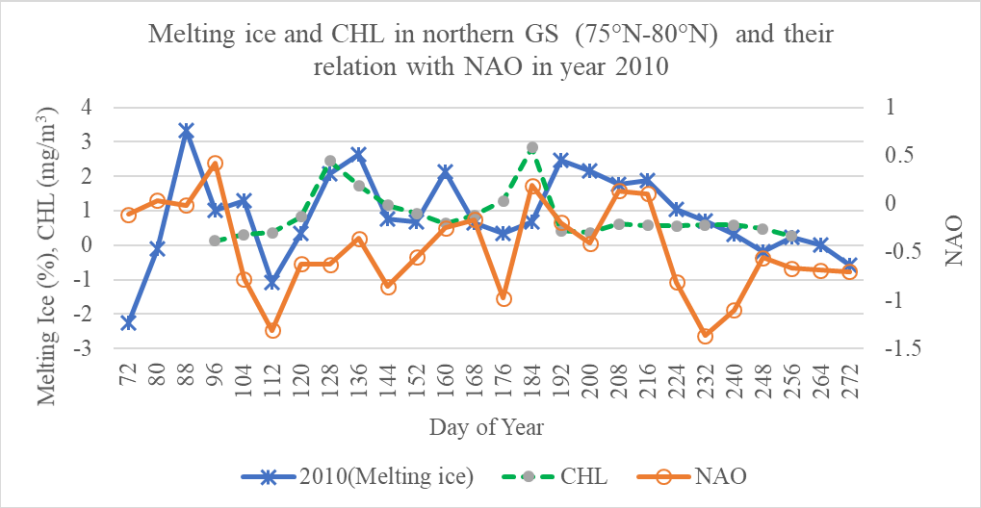

Fig. 12: Spatial average melting ice and CHL in northern GS of year 2010 and comparison with the NAO in year 2010.

4. DISCUSSION

Correlations between spatial averaged ice melt and CHL for both northern BS and GS during springtime (from day 120-168) are shown in (Figure 13). Positive correlations were present for most years in both GS and BS. The positive correlations indicate increased ice melting is associated with higher CHL concentrations in the region for both BS and GS regions. Our results are consistent with our previous studies in GS and BS respectively (Qu et al. 2020, Qu et al. 2016).

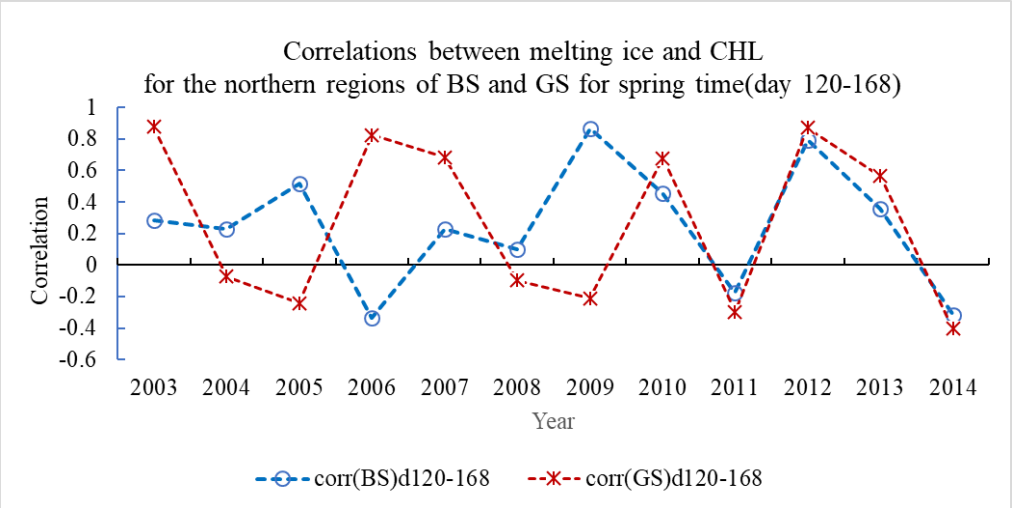

Fig. 13: Correlations between sea ice melt and CHL in northern regions of BS and GS.

In our study region, spatial averaged CHL was much higher in the BS (Figure 2, 3). The elevated spatial average CHL in BS is mainly due to the higher ice melt in northern region (Figure 4) and warmer SST in the southern region (Figure 10). In the GS, spatial average CHL was higher near the western coast (Figure 3). Spatial average CHL blooms in GS are due to several factors: variability in winter ICE and melt water runoff from eastern Greenland Sea (Qu et al. 2018). Eastern Greenland glacial melt water increases the vertical stability of water column and possibly delivers iron and micronutrients which can favor phytoplankton growth (Levasseur 2013).

The satellite derived data used in this study is within a factor of 1.4 of in-situ observations averaged over the optical penetration depth (Bailey and Werdell 2006). Due to cloud and ice cover, the data is more accurate during summertime. Satellite-to-in situ match-ups for MODISA (MODIS instrument on board Aqua) were evaluated for CHL in the western Arctic Ocean, and the errors are well within the range of errors for global data (Chaves et al. 2015).

6. CONCLUSIONS

Decadal spatial average CHL, ICE, SST and NAO in BS and GSa are compared for year 2003-2014. In general, spatial average CHL was higher in BS than GS. High surface CHL were found in 2010 and 2011 in the southern and northern region of BS, while high values were also found in the southern BS in 2013. Due to higher SST in BSS, less ICE occurred in BSS. The peak of CHL was in April or May, but was more than half month earlier in BS, compared with the GS. Compared to the northern region, spatial averaged CHL increased around 77% and 42% in the southern regions of the BS and GS, respectively. The higher SST in the BSS and more melting ice in the BSN are the two major reasons of much higher CHL blooms. Higher CHL blooms in GSN and along the eastern coast of Greenland are mainly caused by the increased ice melting and enriched runoff from glaciers in the east of Greenland to northern and western coastal regions of GS. Earlier and more extensive ice melting and persistent

456 negative NAO index are the possible drivers of higher phytoplankton blooms duri
457 2010.

458 Spatial averaged ICE was generally higher in the western GS than that in the
459 BSN. In the BSN, ICE was high in 2010 and 2013. The peak in SST occurred in
460 August with 2013 having the highest SST over the study time period. Higher SST
461 appeared in the BSS, especially during summer and autumn.

462 The correlations of NAO and spatial average ICE in northern regions are mostly
463 negative. A previous winter negative NAO can correspond to the ICE increase in the
464 following spring. NAO and spatial averaged CHL are mostly negative in spring in GS.
465 The springtime positive NAO indicates a reduced phytoplankton bloom in the
466 springtime in the GS. Melting ice had a positive correlation with CHL in the northern
467 regions, especially in the GS.

468 The relationships between NAO and spatial average ICE, NAO and spatial
469 average CHL were not consistent in the BS, but displayed consistent negative
470 relationships in the GS. However, according to Strong and Magnusdottir (2011), NAO
471 and ICE had negative correlations in BS. The negative correlations of NAO and ICE
472 could be associated with enhanced atmospheric and oceanic heat transport.

473 The GS and BS in Arctic Ocean have significant spatial and interannual
474 differences of ICE and CHL. The structures of their ecosystems are closely related to
475 regional geography, wind, ocean and ice dynamics, and to biogeochemical exchange
476 processes (Carmack and Wassmann 2006). Their ecosystems are tightly connected
477 with physical and biological systems. The ice melt waters mixed with the surface of
478 Atlantic derived warmer waters and then mixing with deeper Arctic colder waters
479 make the study region very dynamic and difficult to draw conclusions for physical
480 and biological systems. The melting ice shifted the polar front northwards (Oziel et al.
481 2017, Oziel, Sirven and Gascard 2016) and shifted phytoplankton blooms a few
482 weeks ahead (Qu et al. 2014, Qu et al. 2006, Qu et al. 2020). Higher spatial averaged
483 CHL in the BS not only related to more ice melting and higher SST, but also sto the
484 particular species of phytoplankton present during different periods. In the BS,
485 diatoms comprise a large fraction during the early stage of ice melt with flagellates

being more important during the late stage (Tamelander et al. 2009). The flagellates correspond with a higher phytoplankton biomass (Wassmann 1999, Tamelander et al. 2009). The loss of sea ice in summer can decrease the surface albedo and increase SST, hence amplifying ocean warming. However, the loss of ice also contributes to increased phytoplankton biomass in the more open upper ocean.

The decline of Arctic sea ice in recent decades has resulted in a regional SST increase of twice the global average rate and is likely to continue to increase throughout this century (Chalecki 2007). Improved understanding of the links between the Arctic ecosystem and food web structure and future climate change may result from progress through the following: the coordination of efforts to more accurately collect and analyse satellite remote sensing data, more extended field data monitoring and more advanced numerical modelling. Moreover, better adaptation and mitigation strategies are expected to be developed, in order to address global warming and other anthropogenic activities which might affect the Arctic Ocean.

DATA AVAILABILITY STATEMENT

The datasets generated and/or analyzed during the current study are available from the corresponding author on reasonable request.

ACKNOWLEDGEMENTS

Sincerely thanks should first go to He-he Li, Xiao Liu and Ai-Lun Fan for their CHL and WIND satellite data retrieving and calculations during year 2003-2014 in Greenland Sea, Barents Sea and the whole study region. Thanks to NASA Ocean Biology Processing Group and Goddard Space Flight Centre of SeaWiFS Project group for providing MODIS CHL data. Thanks to NOAA NCEP EMC CMB GLOBAL Reyn-SmithOIv2 for providing ICE data. Thanks to the Naval Research Laboratory Remote Sensing Division, the Naval Center for Space Technology, and the National Polar-orbiting Operational Environmental Satellite System (NPOESS) for providing WIND, SST data. Thanks NASA Global precipitation Measurement Mission for providing Giovanni Web-based application developed by the Goddard

Earth Sciences Data and Information Services Center (GES DISC), for better image visualizations for CHL, ICE, and SST

Finally, we gratefully acknowledge the Chinese National Natural Science Foundation (Funding No. 41276097) for providing research funding for this project.

References

Acker, J. G. & G. Leptoukh (2007) Online Analysis Enhances Use of NASA Earth Science Data. *Eos Transactions American Geophysical Union* 88**,** 14-17.

Ardyna, M., M. Babin, M. Gosselin, E. Devred, L. Rainville & J.-É. Tremblay (2014) Recent Arctic Ocean sea ice loss triggers novel fall phytoplankton blooms. *Geophysical Research Letters,* 41**,** 6207-6212.

Arrigo, K. R., G. van Dijken & S. Pabi (2008) Impact of a shrinking Arctic ice cover on marine primary production. *Geophysical Research Letters,* 35**,** -.

Bailey, S. & J. Werdell (2006) A multi-sensor approach for the on-orbit validation of ocean color satellite data products. *Remote Sensing of Environment,* 102**,** 12-23.

Budikova, D. (2009) Role of Arctic Sea Ice in Global Atmospheric Circulation: A review. *Global and Planetary Change,* 68 149-163.

Carmack, E. & P. Wassmann (2006) Food webs and physical–biological coupling on pan-Arctic shelves: Unifying concepts and comprehensive perspectives. *Progress in Oceanography,* 71**,** 446-477.

Chalecki, B. (2007) Climate Change in the Arctic and its Implications for U.S. National Security. *Journal of Public & International Affairs,* 18**,** 204-222.

Chaves, J. E., P. J. Werdell, C. W. Proctor, A. R. Neeley, S. A. Freeman, C. S. Thomas & S. B. Hooker (2015) Assessment of ocean color data records from MODIS-Aqua in the western Arctic Ocean. *Deep Sea Research Part II: Topical Studies in Oceanography,* 118, Part A**,** 32-43.

D'Andrea, F., A. Czaja & J. Marshall (2005) Impact of Anomalous Ocean Heat Transport on the North Atlantic Oscillation. *Journal of Climate,* 18**,** 4955-4969.

Dalpadado, P., K. R. Arrigo, S. S. Hjøllo, F. Rey, R. B. Ingvaldsen, E. Sperfeld, G. L. van Dijken, L. C. Stige, A. Olsen & G. Ottersen (2014) Productivity in the Barents Sea - Response to Recent Climate Variability. *PLOS ONE,* 9**,** e95273.

Dickman, M. D. 1998. Hong Kong's worst red tide. In *Proc. Int. Symp. Env. Hydraulics,* 641-645. Hong Kong Observatory: Balkema.

Engelsen, O., E. N. Hegseth, H. Hop, E. Hansen & S. Falk-Petersen (2002) Spatial variability of chlorophyll-a in the Marginal Ice Zone of the Barents Sea, with relations to sea ice and oceanographic conditions. *Journal of Marine Systems,* 35**,** 79-97.

Glowienka-Hense, R. (1985) Studies on the variability of Icelandic Low and Azores High between 1881-1983. *Contrib Atmos Phys,* 58**,** 160-170.

Gradinger, R. R. & M. E. M. Baumann (1991) Distribution of phytoplankton

communities in relation to the large-scale hydrographical regime in the Fram Strait. *Marine Biology,* 111**,** 311-321.

Harris, C. L., A. J. Plueddemann & G. G. Gawarkiewicz (1998) Water mass distribution and polar front structure in the western Barents Sea. *Journal of Geophysical Research: Oceans,* 103**,** 2905-2917.

Hegseth, E. (1997) Phytoplankton of the Barents Sea -- The end of a growth season. *Polar Biology,* 17**,** 235-241.

Holland, M. M., C. M. Bitz, and B. Tremblay (2006) Future abrupt reductions in the summer Arctic sea ice. *Geophys. Res. Lett.,* 33**,** L23503

Hurrell, J. W. (1996) Influence of variations in extratropical wintertime teleconnections on northern hemisphere temperature. *Geophysical Research Letters,* 23**,** 665-668.

Hurrell, J. W. 2000. The North Atlantic Oscillation. In *12th Annual Symposium on Frontiers of Science*. Irvine, CA.

Hurrell, J. W. & C. Deser (2009) North Atlantic climate variability: The role of the North Atlantic Oscillation. *Journal of Marine Systems,* 78**,** 28-41.

Irigoien, X., R. P. Harris, R. N. Head & D. Harbour (2000) North Atlantic Oscillation and spring bloom phytoplankton composition in the English Channel. *Journal of Plankton Research,* 22**,** 2367-2371.

Kogeler, J. & F. Rey (1999) Ocean colour and the spatial and seasonal distribution of phytoplankton in the Barents Sea. *International Journal of Remote Sensing,* 20**,** 1303-1318.

Lara, R. J., G. Kattner, U. Tillmann, H. J. Hirche (1994) The North East Water polynya (Greenland Sea) II. Mechanisms of nutrient supply and influence on phytoplankton distribution. *Polar Biol. ,* 14**,** 483-490.

Levasseur, M. (2013) Impact of Arctic meltdown on microbial cycling of sulphur. *Nat. Geosci,* 6**,** 691-700.

Liu, J., J. A. Curry & Y. Hu (2004) Recent Arctic Sea Ice Variability: Connections to the Arctic Oscillation and the ENSO. *Geophysical Research Letters,* 31.

Loeng, H. (1991) Feature of the physical oceanographic conditions of the Barents Sea. *Polar Research,* 10**,** 5-18.

Marshall, J., H. Johnson & J. Goodman (2001) A Study of the Interaction of the North Atlantic Oscillation with Ocean Circulation. *Journal of Climate,* 14**,** 1399-1421.

Moline, M. A., N. J. Karnovsky, Z. Brown, G. J. Divoky, T. K. Frazer, C. A. Jacoby, J. J. Torres & W. R. Fraser (2008) High Latitude Changes in Ice Dynamics and Their Impact on Polar Marine Ecosystems. *Annals of the New York Academy of Sciences,* 1134**,** 267-319.

Neukermans, G., L. Oziel & M. Babin (2018) Increased intrusion of warming Atlantic water leads to rapid expansion of temperate phytoplankton in the Arctic. *Global Change Biology,* 24.

Oziel, L., G. Neukermans, M. Ardyna, C. Lancelot, J.-L. Tison, P. Wassmann, J. Sirven, D. Ruiz-Pino & J.-C. Gascard (2017) Role for Atlantic inflows and sea

ice loss on shifting phytoplankton blooms in the Barents Sea. *Journal of Geophysical Research: Oceans,* 122**,** 5121-5139.
Oziel, L., J. Sirven & J. C. Gascard (2016) The Barents Sea frontal zones and water masses variability (1980–2011). *Ocean Sci.,* 12**,** 169-184.
Pang, H. 2006. *Econometrics*. Beijing: Science Press.
Qu, B., A. J. Gabric, H. Lu & D. Lin (2014) Spike in phytoplankton biomass in Greenland Sea during 2009 and the correlations among chlorophyll-a, aerosol optical depth and ice cover. *Chinese Journal of Oceanology and Limnology,* 32**,** 241-254.
Qu, B., A. J. Gabric, Z. Lu, H. Li & L. Zhao (2016) Unusual phytoplankton bloom phenology in the northern Greenland Sea during 2010. *Journal of Marine Systems,* 2164**,** 144-150.
Qu, B., A. J. Gabric & a. P. A. Matrai. (2006) The Satellite-Derived Distribution of Chlorophyll-a and its Relation to Ice Cover, Radiation and Sea Surface Temperature in the Barents Sea. *Polar Biology,* 29.
Qu, B., A. J. Gabric, M. Zeng & X. Liu (2020) Correlations among Phytoplankton biomass, Sea ice and Wind Speed in Barents Sea and the future climate trends. *Polar Science,* 24**,** 100525.
Qu, B., A. J. Gabric, L. Zhao, W. Sun, Li，H.;, P. Gu & Zeng, M. (2018) The relationships among aerosol optical depth, ice, phytoplankton and dimethylsulfide and the implication for future climate in the Greenland Sea. *Acta Oceanologica Sinica,* 37**,** 13-21.
Rey, F., T. T. Noji & L. A. and Mille (2000) Seasonal phytoplankton development and new production in the central Greenland Sea. *Sarsia,* 85**,** 329-344.
Reynolds, R. W., N.A. Rayner, T.M. Smith, D.C. Stokes, and W. Wang (2002) An Improved In Situ and Satellite SST Analysis for Climate. *J. Climate,* 15**,** 1609-1625.
Signorini, S. & C. McClain (2009) Environmental factors controlling the Barents Sea spring-summer phytoplankton blooms. *Geophysical Research Letters - GEOPHYS RES LETT,* 36.
Slagstad, D., I. H. Ellingsen & P. Wassmann (2011) Evaluating primary and secondary production in an Arctic Ocean void of summer sea ice: An experimental simulation approach. *Progress In Oceanography,* 90**,** 117-131.
Slagstad, D. & K. Stole-Hansen (1991) Dynamics of plankton growth in the Barents Sea: model studies. *Polar Research. ,* 10**,** 173-186.
Spies, A. (1987) Phytoplankton in the marginal ice zone of the Greenland Sea during summer, 1984. *Polar biology,* 7**,** 195-205.
Stroeve, J., M. M. Holland, W. Meier, T. Scambos & M. Serreze (2007) Arctic sea ice decline: Faster than forecast. *Geophysical Research Letters,* 34**,** L09501.
Strong, C. & G. Magnusdottir (2011) Dependence of NAO variability on coupling with sea ice. *Climate Dynamics,* 36**,** 1681-1689.
Struthers, H., A. M. L. Ekman, P. Glantz, T. Iversen, A. Kirkevåg, E. M. Mårtensson, Ø. Seland & E. D. Nilsson (2011) The effect of sea ice loss on sea salt aerosol concentrations and the radiative balance in the Arctic. *Atmos. Chem. Phys.,* 11**,**

3459-3477.
Tamelander, T., M. Reigstad, T. Ratkova & H. Hop (2009) Ice algal assemblages and vertical export of organic matter from sea ice in the Barents Sea and Nansen Basin (Arctic Ocean). *Polar Biol.,* 32**,** 1261-1273.
van den Dool, H. M., S. Saha & Å. Johansson (2000) Empirical Orthogonal Teleconnections. *Journal of Climate,* 13**,** 1421-1435.
Wang, J. & M. Ikeda (2000) Arctic oscillation and Arctic sea-ice oscillation. *Geophysical Research Letters,* 27**,** 1287-1290.
Wassmann, P., Ratkova, T, Andreassen, I, Vernet, M, Pedersen, C, Rey, F (1999) Spring bloom development in the marginal ice zone and the central Barents Sea. *Marine Ecology,* 20**,** 321-346.
Wassmann, P., M. Reigstad, T. Haug, B. Rudels, M. Carroll, H. Hop, G. Gabrielsen, S. Falk-Petersen, S. Denisenko, E. Arashkevich, D. Slagstad & O. Pavlova (2006) Food webs and carbon flux in the Barents Sea. *Progress In Oceanography,* 71**,** 232-287.
Yamamoto, K., Tachibana, Y., Honda, M., and Ukita (2006) Intra‐seasonal relationship between the Northern Hemisphere sea ice variability and the North Atlantic Oscillation. *J. Geophys. Res. Lett.,* 33**,** L14711.
Zhang, X. & J. E. Walsh (2006) Toward a Seasonally Ice-Covered Arctic Ocean: Scenarios from the IPCC AR4 Model Simulations. *Journal of Climate*.